Available online at www.sciencedirect.com
ScienceDirect
Journal of the European Ceramic Society 31 (2011) 697–703
www.elsevier.com/locate/jeurceramsoc

Dynamic corrosion of Al_2O_3–ZrO_2–SiO_2 and Cr_2O_3-containing refractories by molten frits. Part I: Macroscopic analysis

C. Baudín [a], E. Criado [a], J.J. Bakali [b,1], P. Pena [a,*]

[a] *Instituto de Cerámica y Vidrio, CSIC, Kelsen 5, 28049 Madrid, Spain*
[b] *Esmaltes S.A., Ctra. Castellón km 22, 5, 12110 LiAlcora, Castellón, Spain*

Available online 18 December 2010

Abstract

Manufacturing of enamels and frits has undergone dramatic changes since the 1980s. This has required significant efforts in research and development. Typical compositions of frits for ceramic tiles are silica-based with fluxing agents; some of the components are highly corrosive. Improvements in the production of frits would imply the selection of the most adequate refractories as a function of the chemical composition of the considered frit and the fabrication procedure.

The refractories currently used in frit furnaces are Al_2O_3–ZrO_2–SiO_2 (AZS) fused cast materials and Cr_2O_3-based materials. In this work, results on dynamic corrosion studies of AZS and Cr_2O_3-based materials by two ZnO-containing frits are described. Experiments have been performed using the "Merry Go Round" test at ≅1500 °C. Macroscopic results are analysed in terms of the remaining volume after the tests, as usually done in the glass industry. The significance and limits of such an approach are discussed.

Keywords: Refractories; Corrosion; Glass; Al_2O_3; Cr_2O_3; ZrO_2

1. Introduction

The tile industry, being dependent on the construction business, has the need to change as a function of customer new demands, or even to create such demands. The aspect of tiles that involves the major activity in research and development is that of enamels and frits, where manufacturing has undergone dramatic changes since the 1980s. Not only the new characteristics of the final product – colours, shines, insulating properties or wear resistance – that are being advanced every day, but also the fast and highly automatic new processes for fabrication of tiles make it necessary to develop new enamel and frit compositions. Moreover, in many cases, the required total production span of a new frit composition is very short, nearly an "ask what you want" fabrication. As a consequence, the producer of frits has to be prepared for a highly variable production style. Finally, the enamel and frit industry is nowadays obliged to account for larger production under more technological requirements such as energy saving and pollution control.

Typically, a frit has a silica-based composition with fluxing agents, namely CaO, PbO, K_2O, Na_2O, and B_2O_3, which allow low temperature fusion, and different amounts of other minor components, ZrO_2, TiO_2, ZnO, Cr_2O_3, and others, to assure specific physical and/or chemical properties. As a consequence, the nature and specific quantity of all these oxides depend on the envisaged requirements for the frit.

As a broad classification, frits are divided into two large groups: crystalline (or transparent) and white. There is also used a subdivision of crystalline frits into high temperature (HTF) and low temperature (LTF). The crystalline frits, and specifically those designed for tile production at the lowest temperatures (LTF), have the most corrosive compositions.

In all applications, the refractories must guarantee a sufficient, i.e., economically feasible-lifetime. Nevertheless, the basic requirements for the production of glass are refractories that do not affect the quality of the product.[1] In particular, coloration is a fundamental technical problem. On the contrary, as natural raw materials such as kaolin, with minor amounts of colorant impurities, are added to frits to fabricate the enamels and constitute the tile substrate, coloration is not such an extreme requirement in frits as, for instance, in soda-lime glass for windows.[2,3] The critical factor in frit production would be the life of the furnace, which is subjected to the extremely corro-

* Corresponding author.
E-mail address: ppena@icv.csic.es (P. Pena).
[1] Actual address: Parque Lidón, Torre 4, 8°B, 12003 Castellón, Spain.

0955-2219/$ – see front matter © 2010 Elsevier Ltd. All rights reserved.
doi:10.1016/j.jeurceramsoc.2010.11.023

sive and variable environment originated by the components of the frits. In spite of this, very little work has been done to understand the corrosion process of refractories by frits, to allow the design of best refractory distribution as a function of the area of the furnace in order to maximize its life. In fact, most fabricants have been assuming the high consumption of refractories as intrinsic for frit production.

Not only the increasing prices of refractories and furnace repairs, but also the new environmental regulations about waste, and the need of more performing and environmentally friendly fabrication processes, require the building up of basic understanding on refractory corrosion by frits.

The considered refractories currently used in glass and frit furnaces are Al_2O_3–ZrO_2–SiO_2 (hereafter termed AZS) fused cast refractory materials and Cr_2O_3-based materials. AZS and high chromic oxide refractories have been used for over 40 years as glass contact refractories in glass melting furnaces, mainly for high corrosive glass compositions and critical areas in the glass furnaces: throat, flux line area, doghouse corner blocks or feeders.[2,3] Products typically used in container thank high wear areas include fused AZS with 36 wt.% and 40 wt.% ZrO_2 and bonded products containing more than 80 wt.% of Cr_2O_3. The corrosion resistance of fused AZS is often less than that required in high wear areas of glass furnaces. Dynamic corrosion tests have proved the high corrosion resistance of high-chromia refractories by soda-lime glasses at 1450 and 1550 °C.[2,3]

Against this background, the objective of this work has been to analyse the corrosion process of four commercial refractories by two different crystalline frits, with characteristic compositions of low and high temperature (LTF, HTF) types. Two refractories of each quality, AZS and Cr_2O_3-based, have been chosen to determine the basic mechanisms as well as the influence of microstructural features on corrosion.

The "Merry Go Round" test, currently used in the glass industry, has been chosen for corrosion. In this test, four refractory specimens are immersed in a large crucible filled with the melt and rotating. Therefore, this test involves dynamic contact between the refractory and the melt, as occurs in frit melting furnaces. After the test, the remaining volume of each sample is determined and the products are ranked according to a product standard. In general, this ranking allows the selection of the most resistant refractory products to be proposed for industrial applications with the very best chance of optimum performance.

In the first part of the work, macroscopic results are analysed in the same way as they are in the glass industry, and the significance and limits of such approach are discussed. In the second part,[4] the microstructural study of corroded specimens is presented and the corrosion mechanisms are described and discussed.

2. Experimental

Four different commercial refractories were studied, two electrofused AZS (AZS1681 and AZS1711, Saint Gobain, France) and two Cr_2O_3-based (CR-95WB and ZC-85, Dyko Vesuvius, Germany). Main physical and chemical characteristics are given in Table 1. Two different crystalline frits, one for high and the other for low temperature applications, which will be named HTF and LFT, were used for the tests. Average compositions for the studied frits are given in Table 2. The chemical analyses of the Cr_2O_3-based refractories and the frits were carried out by X-ray fluorescence spectroscopy (XRF, Magi X; Phillips, The Netherlands) and flame emission spectrometry for alkaline analyses (Na and K) (FES, 2100; Perkin Elmer).

Table 1
Chemical composition (wt.%) and physical properties of the refractory materials.

Chemical composition (wt.%)	Material			
	AZS1681[a]	AZS1711[a]	CR-95WB[b]	ZC-85[b]
SiO_2	15	12	1.52	1.26
Al_2O_3	50.9	46.7	0.20	2.53
ZrO_2	32.5	40.0	0.03	8.65
Na_2O	1.3	1.1	n.d.	0.21
Others	0.3	0.2	0.12	0.8
Cr_2O_3	n.d.	n.d.	95.4	84.9
TiO_2	n.d.	0.12	2.62	1.59
CaO	n.d.	n.d.	0.02	0.56
Mineralogy[c]	α-Al_2O_3 m-ZrO_2 Glass	α-Al_2O_3 m-ZrO_2 Glass	Cr_2O_3	Cr_2O_3 m-ZrO_2 $ZrTiO_4$
Density[c]	3.84	4.09	4.11	4.05
Open porosity (%)[c]	≅1.5	≅1.5	15.9 ± 0.1	17.0 ± 0.1

[a] Saint Gobain (France). Catalogue data.
[b] Dyko Vesuvius (Germany). Catalogue data.
[c] Present work.

2.1. Microstructural characterisation of the "as received" materials

The crystalline phases present in the materials after grinding were analysed by X-ray diffraction (XRD). XRD patterns were recorded on an automated diffractometer Siemens D5000 using Cu $K_{\alpha 1,2}$ radiations (1.5418 Å) and a secondary curved graphite monochromator. The data were collected in the Bragg–Brentano ($\theta/2\theta$) vertical geometry (flat reflection mode) between 2° and 60° (2θ) in 0.05° steps, counting for 1.5 s per step. The sample was rotated at 15 r min^{-1} during the acquisition of patterns to improve the powder averaging. The diffraction patterns were compared to the ASTM files (86-1451, 46-1212, 84-313 and

Table 2
Average chemical composition of the frits used for the corrosion tests. LTF: low temperature frit; HTF: high temperature frit.[a]

Oxide	wt. (%)	
	LTF	HTF
SiO_2	61	63
Al_2O_3	8.6	7.0
B_2O_3	8.5	1.5
CaO	10	15
ZnO	3.5	8.6
K_2O	4.7	3.5
Na_2O	3.4	0.4
Others	0.3	1

[a] Esmaltes S.A.

Fig. 1. Specially developed apparatus for the "Merry go Round test", used in this work. The mullite plate used as top of the rotary furnace is slightly elevated to show the arrangement of the four test specimens. The crucible is filled with the molten frit.

Fig. 2. Mullite plate used as top of the rotary furnace in the specially developed apparatus for the "Merry go Round test" (Fig. 1), before the test. The arrangement of the test specimens (black: cromite, white: electrofused) and the four holes for the burners are observed.

34-415), for monoclinic ZrO_2, α-alumina, Cr_2O_3 and $ZrTiO_4$, respectively.

Diamond polished surfaces of the materials were characterised by reflected light optical microscopy (RLOM, Model HP 1, Carl Zeiss, Oberköchen and Jena Gmb, Germany) and scanning electron microscopy with energy dispersive X-ray spectroscopy (SEM-EDX, Model DSM 950, Karl Zeiss, Thornwood, NY; series, Tracor Northern, Middleton, WI). Microchemical analyses were carried out by EDX (counting time = 60 s) to determine the composition of the observed phases. Semiquantitative analyses were done using ZAF (atomic number, absorption, fluorescence) and corrected by the software provided with the equipment.

2.2. Corrosion test

Fig. 1 shows the specially developed apparatus for the "Merry go Round test" used in this work (Centro de Investigación y Desarrollo, Saint Gobain, Avilés, Spain). A rotating cylindrical furnace of 220 mm internal diameter and 155 mm internal height, made of sillimanite, was filled with frit to reach 120 mm height once melted, which corresponded to a total volume of frit of about 4.6 l. A silico-aluminate plate, with four holes to place the test pieces and four additional ones to introduce the natural gas burners, was used as top of the furnace (Figs. 1 and 2). Four test pieces, one of each studied refractory, in the shape of cylinders of 120 mm length and 20 mm diameter ("fingers") were placed in the corresponding holes and fixed by means of refractory cement (Fig. 2). During the test, the top was fixed at about 2–3 mm above the furnace and this latter turned at 6 rpm. Rotation of the furnace avoids the formation of films saturated by reaction products between the fingers and the frit. After 24 h of test, the superstructure was taken off and left to cool at room temperature. Then, half of the molten frit was taken off and the crucible was filled again with un-melted frit and left to melt. Once the frit had melted, a new top with another four fingers (Fig. 2) was set in place and the test ran again for 24 h. In this way, results for two test pieces of each studied material were analysed.

Temperature control was done by means of a thermocouple placed inside the mullite plate and the direct measurement of the temperature of the surface of the molten frit was done with an optical pyrometer. For this latter, the top has to be slightly elevated as shown in Fig. 1. The testing temperatures during the whole testing periods were fairly coincident for both frits. They were in the ranges $1660 \pm 20\,^{\circ}C$ and $1510 \pm 10\,^{\circ}C$ for the mullite top and for the melt, respectively.

In order to evaluate the remaining volume of the corroded fingers, they were immersed in an index fluid (20 vol.% tryacetyl glycerine and 80 vol.% benzyl alcohol) and photographed. The selected index fluid had similar refraction index to those of the solid frits attached to the test pieces. Thus, the photographs could be analysed by image analysis to determine the remaining surface of refractory as indirect evaluation of the remaining volume.

In the glass industry, the test piece presenting the highest corrosion is selected as reference in order to compare quantitatively the results of the corrosion tests. In this work, in order to compare not only the different materials but also the relative effect of the different frits, the result for the combination of material and frit for the conditions of maximum corrosion (specimen 1681 tested using the LTF) was used as reference (corrosion index = 1).

The corrosion index for one piece was defined as:

$$\text{Corrosion index for test piece } A = \frac{(s_r/s_i)_A}{(s_r/s_i)_R}$$

where s_r and s_i are the remaining and initial areas of the test pieces in the photographs, respectively, and A and R stand for the considered piece and reference piece, respectively.

The average of the results for the remaining surface, s_r, of the two fingers tested for each material was taken to calculate the corrosion index.

Such an analysis of the corrosion results gives the relative performance of the different materials under the conditions tested as compared with the "worst case scenario" and is used in the glass industry to select the most adequate materials for the specific locations in the furnace.

2.3. Characterisation of the frits

The viscosity of the frits at the testing temperature (≅1500 °C) was determined using a high temperature rotation viscosimeter of the cylindrical Searlex type, at rotation speeds 1–30 rpm for 10 min.[5]

In order to evaluate the possibility of extreme frit coloration due to the interaction of the Cr_2O_3 refractories and the frits, the chemical compositions of the LTF before testing and that of the remaining frit after 24 and 48 h test were determined by X-ray fluorescence (XRF, Magic X PW2424 Philips, The Netherlands), atomic absorption spectrometry in the flame emission mode (FES, Perkin–Elmer, USA) for alkalis, and plasma spectrometry (Jarrel Ash Iris Advantage, USA) for B_2O_3.

3. Results and discussion

3.1. Refractory materials

Fig. 3 summarises the main microstructural characteristics of the AZS electrofused refractories. The microstructures of both materials (Fig. 3a–b) consisted of interlocking alumina–zirconia eutectic polycrystals, glassy phase (wt.% ≈: 70 SiO_2, 20 Al_2O_3, 5 Na_2O and 2 ZrO_2, according to SEM-EDS analysis) and the almost insoluble primary ZrO_2 crystals dispersed in the glassy phase. The eutectic structure was formed by small (≈10 μm) ZrO_2 particles surrounded by alumina. The sizes of the primary ZrO_2 particles were larger (>40 μm). Such microstructures led to extremely low levels of porosity (≈1.5%, Table 1). The amount and the particle size of the primary zirconia in AZS materials are determined by the location of their compositions in the ternary phase equilibrium diagram Al_2O_3–ZrO_2–SiO_2. In Fig. 3c, the compositions of the studied AZS refractories (Table 1) are plotted. From this diagram, material AZS1681 would have a lower proportion of smaller primary zirconia particles than AZS1711, as qualitatively observed in Fig. 3a–b. On the other hand, significant amounts of glass were present in both materials due to the fabrication procedure.

As expected, the major crystalline component of the Cr_2O_3 refractories was a Cr_2O_3 (Table 1). Typical impurities in the Cr_2O_3 aggregates, TiO_2 and SiO_2, were present in both materials (Table 1). In general, TiO_2 will be in solid solution in the Cr_2O_3 crystalline structure whereas SiO_2 will form residual glass. Monoclinic ZrO_2 as minor crystalline phase and traces of $ZrTiO_4$ were also present in one of them (ZC-85), in agreement with the amount of ZrO_2 determined by chemical analysis (Table 1). In this latter material, the amount of minor impurities (≈4 wt.%) was much higher than in CR-95WB (≈0.3 wt.%).

As shown in Fig. 4, the microstructures of both materials were mainly constituted by Cr_2O_3 aggregates with sizes up to 2000 μm with small pores (<20 μm) at the grain boundaries

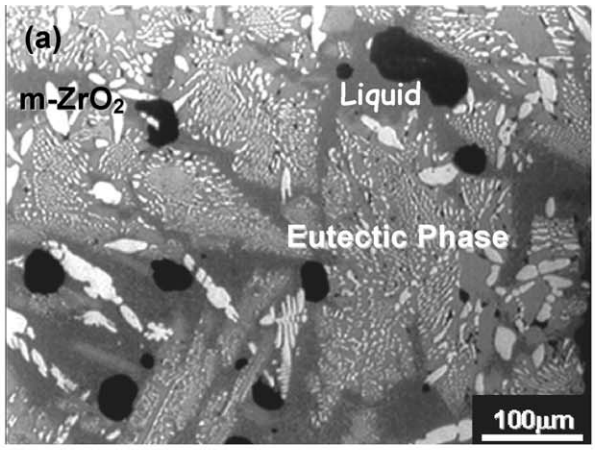

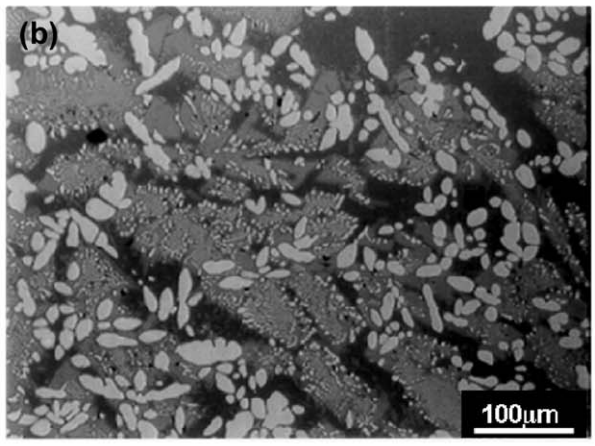

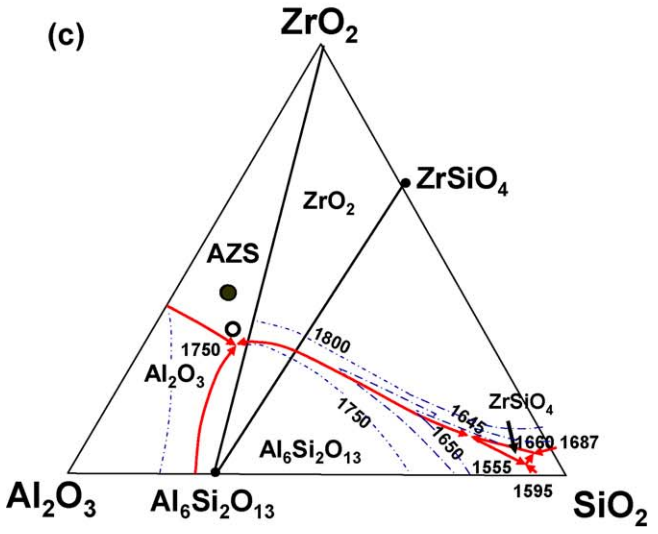

Fig. 3. Microstructural characteristics of the electrofused AZS refractories. (a and b) Reflected light optical microscopy micrographs of polished surfaces. The eutectic phase constituted by alumina (grey) and zirconia (white) is surrounded by glass in which primary zirconia particles are located. (a) Material with 36 wt.% of ZrO_2 (AZS1681). (b) Material with 40 wt.% of ZrO_2 (AZS1711). (c) Ternary Al_2O_3–ZrO_2–SiO_2 phase equilibrium diagram with the compositions of the studied materials plotted. From the composition corresponding to AZS1681 less amount of primary zirconia will be present than in refractory AZS1711. The solid circle corresponds to AZS1711 and the hollow circle to AZS1681.

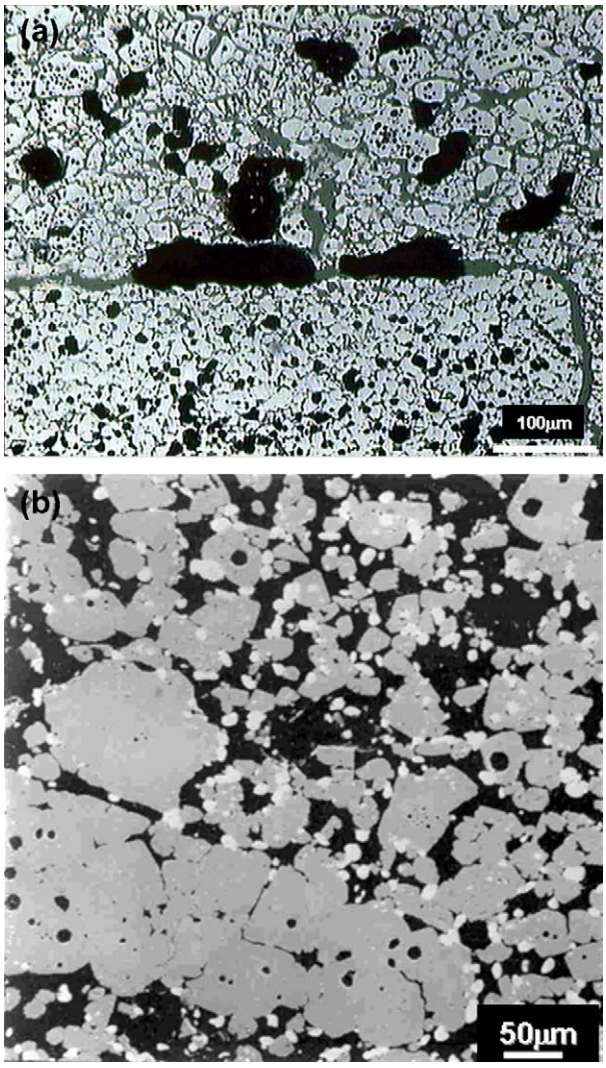

Fig. 4. Microstructural characteristics of the Cr_2O_3-based refractories. Micrographs of polished surfaces. The light grey particles are Cr_2O_3 and the pores are black. (a) Material with 96 wt.% of Cr_2O_3 (CR-95WB). The Cr_2O_3 aggregates are bonded by a matrix formed fine by Cr_2O_3 particles. Reflected light optical microscopy. (b) Material with 84 wt.% of Cr_2O_3 (ZC-85). The Cr_2O_3 aggregates are bonded by a matrix (dark grey). The composition of the matrix was identified by SEM-EDS as silica glass and zirconia. The ZrO_2 particles (white) are observed bonding the Cr_2O_3 aggregates. Scanning electron microscopy.

and triple points of the Cr_2O_3 grains. Significant amounts of large (>100 μm) pores between the aggregates were observed. The large elongated pores observed in the microstructures corresponded to the high levels of open porosity determined for these materials (Table 1). In the material with the highest amount of Cr_2O_3, the aggregates were bonded by fine Cr_2O_3 grains (Fig. 4a). In the other material, the matrix was constituted by fine Cr_2O_3 grains bonded by ZrO_2 and residual glass (Fig. 4b). The significant amount of minor impurities in the materials should be located in the residual glass.

3.2. Characterisation of the frits

Table 2 summarises the chemical compositions of the frits used for the corrosion testing. The major constituent of both frits

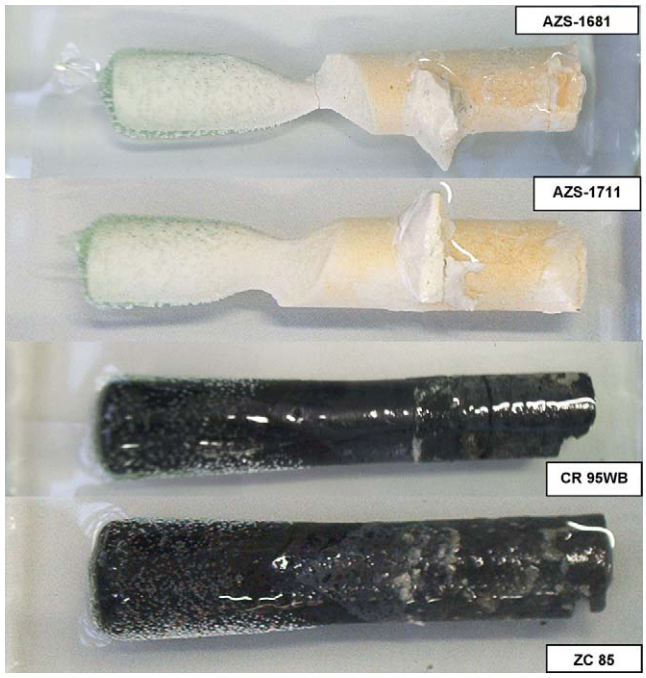

Fig. 5. Aspect of the tested specimens (≅1500 °C-24 h) after immersion in the index liquid. The remaining part of the samples is observed. The extension of corrosion at the triple point (solid–liquid–gas) is observed. The electrofused AZS refractories show much frit (HTF).

was SiO_2 and main differences between their chemical compositions were the nature and amount of the fluxing agents, namely CaO, K_2O, Na_2O, and B_2O_3 and the amount of ZnO. The low temperature frit (LTF) had the largest amount of B_2O_3, K_2O and Na_2O whereas the high temperature one had significantly larger amount of ZnO. Both frits were completely melted at the testing temperature (≅1500 °C) with viscosities $\log\eta = 2.1$ and 2.2 (η in Pa s) for the LTF and HTF, respectively. These values were in agreement with the respective B_2O_3 contents (Table 2), as this compound is a determining factor for low glass viscosity.[6]

3.3. Corrosion tests

The frit temperatures during the whole testing periods were fairly coincident for both frits (1510 ± 10 °C), as a consequence, the viscosity of the LTF was slightly lower than that of the HTF during the whole testing period.

Fig. 5 shows the aspect of the tested specimens submerged in the index liquid, the remaining part of the refractory was easily distinguished once the optical effect of the frit, glued to the specimens after cooling from testing, was eliminated by the index liquid. At first sight, the severe corrosion experienced by the electrofused materials as compared to both Cr_2O_3-based ones is apparent.

In the photographs of the electrofused samples it is clearly observed the spiral corrosion, as shown by the oblique triple point profiles (Fig. 5). This is a specific characteristic of this kind of tests as the flow velocity of the melt at the inner part of the tank is slower than at the outer circle. Therefore, the effect of the melt is more severe at the zones of the fingers closer to the outer circle.

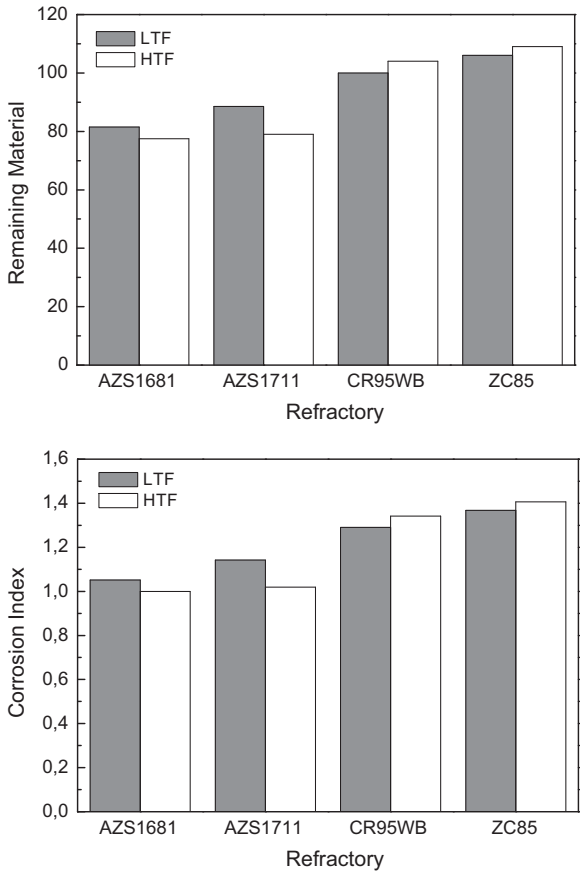

Fig. 6. Summary of macroscopic results of the corrosion test (≅1500 °C-24 h). LTF and HTF correspond to low and high temperature frits, respectively. (a) Corrosion index according to the standard method. Reference (corrosion index = 100) was material AZS1681 after testing with the LTF. (b) Remaining material as a percentage of the initial sample volume. The expansion of the Cr_2O_3-based materials is clearly observed.

For both frits, the specimens that showed the largest corrosion were those of AZS1681, and the largest extent of corrosion occurred during the tests with the HTF, therefore, values for AZS1681 specimens after testing with the HTF were taken as reference (corrosion index = 1). In Fig. 6a, results for corrosion index are summarised. Such representation reveals the relative performance of refractories, better as the corresponding index is higher than 1. On the contrary, no definite trend can be drawn about the relative corrosive power of the studied frits, as the tendency changes with the chemical nature of the material.

The corrosion results are plotted as percentage of remaining material in Fig. 6b in order to highlight an important result referring to the Cr_2O_3-based materials. In spite of the slight increase of Cr_2O_3 content in the frit during the tests (Table 3), which would indicate partial dissolution of the refractory into the frit, the remaining parts of the Cr_2O_3-based specimens were larger than the initial fingers. Thus, expansion of the specimens occurred during the corrosion tests. Therefore, corrosion in these materials was associated with expansive reactions between the frit and the refractory. This result demonstrates that the macroscopic analysis has limited prediction capacity when extremely different materials such as those studied here are compared.

Table 3
Comparison between the original composition the LTF and the composition after 24 and 48 h corrosion test. Errors stand for the standard deviation of five determinations on different samples.

Components	Original	24 h	48 h
SiO_2	60.2 ± 0.4	60.4 ± 0.4	61.1 ± 0.4
Al_2O_3	8.40 ± 0.06	8.90 ± 0.06	9.55 ± 0.06
CaO	9.70 ± 0.06	9.75 ± 0.06	9.70 ± 0.06
Na_2O	3.6 ± 0.1	3.4 ± 0.1	3.0 ± 0.1
K_2O	4.80 ± 0.08	4.29 ± 0.08	4.05 ± 0.08
ZnO	3.90 ± 0.05	3.76 ± 0.05	3.40 ± 0.05
MgO	0.070 ± 0.02	0.063 ± 0.02	0.064 ± 0.02
P_2O_5	0.052 ± 0.006	0.039 ± 0.006	0.033 ± 0.006
SO_3	0.021 ± 0.005	0.021 ± 0.005	0.016 ± 0.005
TiO_2	0.050 ± 0.006	0.050 ± 0.006	0.042 ± 0.006
Fe_2O_3	0.078 ± 0.005	0.080 ± 0.005	0.11 ± 0.06
Rb_2O	0.017	0.011	0.012
SrO	0.012	0.013	0.011
Y_2O_3	0.0015	0.015	0.011
ZrO_2	0.032 ± 0.005	0.190 ± 0.008	0.310 ± 0.009
BaO	0.065	0.080	0.067
PbO	0.0083	0.010	0.011
Cr_2O_3	<0.005	0.012	0.018
B_2O_3	9.24	9.05	9.10

Even though the macroscopic results shown in Figs. 5 and 6 do not refer to the specific corrosion mechanisms, there are some characteristics of the corrosion process that can be inferred. First, the extent of corrosion experienced by the electrofused materials when tested with the HTF, with higher viscosity, was larger than when the frit was the LTF. Conversely, corrosion by the LTF was higher for the Cr_2O_3-based specimens. These observations indicate that capillary penetration of the frit was not the corrosion rate determining factor for the former materials but could be the determining corrosion factor for the latter ones. The origin of such differences can be related with the microstructural characteristics of the refractories. Corrosion in the electrofused materials (Fig. 3, Table 1), with very low levels of open porosity, would be determined by the progression of reactions at the contact zone between the external surface of the refractory and the frit. Conversely, capillar penetration through the open pores of the Cr_2O_3-based materials would be the primary factor for the increase of the reaction between the frit and these porous materials (Fig. 4, Table 1).

In the experimental conditions used in this work – large residence times, small ratio frit volume/refractory surface and no formation of saturated films at the refractory-frit interface – there is a non-negligible increase of Cr_2O_3 content in the frit. Nevertheless, the standard residence times in the conventional frit furnaces are always lower than 2 h. Consequently, coloration does not appear to be a limiting problem for the application of Cr_2O_3 based materials in these furnaces.

4. Final considerations

The results obtained from the macroscopic analysis of refractory specimens tested using the "Merry Go Round" tests would indicate the better performance of Cr_2O_3 containing refractories in terms of corrosion resistance by frits. However, there are some

aspect that cannot be explained at this point and, therefore, limit the validity of these preliminary conclusions. In fact, the volume increase experienced by the Cr_2O_3-based materials is not understood and might indicate the occurrence of undesired reactions between the frit and the components of the refractory. In order to establish the specific effects of the studied frits on each kind of material, the microstructural analysis of the frit-refractory interfaces in corroded specimens was done and is reported in Part II of this work.[4]

Acknowledgements

In memoriam of Carlos Fueyo.

The authors acknowledge the financial support of CDTI Project number 01-0389 and MCI MAT2009-14448. We thank Vesuvius-VGT-Dyko (Düsseldorf, Germany) and Saint Gobain (France) for kindly supplying the refractory materials used in this work. The authors wish to thank Dr. F.J. Valle for assistance with chemical analyses and Mrs. M. J. Mari Juan for collaboration in corrosion studies.

References

1. Dunkl M. Corrosion tests—a very important investigation method for the selection of refractories for glass tanks. *Glastech Ber Glass Sci Technol* 1994;**67**(12):325–34.
2. Beerkens R, van Dijk F, Dunkl M. Reactions and interactions between tank refractory and glass melt. *Glass Sci Technol Suppl C* 2004;**77**: 35–51.
3. Guigonis J, Larry J, McGarry C, Nelson M. Glass contact application of high-chrome refractories in soda-lime glass melters. In: Kieffer J, editor. Proceedings of the 62nd conference on glass problems. Ceramic Engineering and Science, vol. 23(1). The American Ceramic Society: USA; 2002. p. 193–210.
4. Pena P, Criado E, Bakali J, Baudín C. Dynamic corrosion of Al_2O_3–ZrO_2–SiO_2 and Cr_2O_3-containing refractories by molten frits. Part II: microstructural study. *J Eur Ceram Soc* 2011;**31**:705–14.
5. Pascual MJ, Pascual L, Duran A. Determination of the viscosity–temperature curve for glasses on the basis of fixed viscosity points determined by hot stage microscopy. *Phys Chem Glasses* 2001;**42**(1): 61–6.
6. Fernández-Navarro, JM. In: El Vidrio, editor. Consejo Superior de Investigaciones Científicas, Spain. 3rd. ed.; 2003. p. 314–334 [chapter IV].